NASA/CR-2003-212674

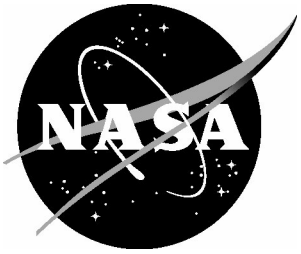

Sound Generation by Aircraft Wake Vortices

Jay C. Hardin
Titan Corporation, Billerica, Massachusetts

Frank Y. Wang
Volpe National Transportation Systems Center, Cambridge, Massachusetts

December 2003

The NASA STI Program Office . . . in Profile

Since its founding, NASA has been dedicated to the advancement of aeronautics and space science. The NASA Scientific and Technical Information (STI) Program Office plays a key part in helping NASA maintain this important role.

The NASA STI Program Office is operated by Langley Research Center, the lead center for NASA's scientific and technical information. The NASA STI Program Office provides access to the NASA STI Database, the largest collection of aeronautical and space science STI in the world. The Program Office is also NASA's institutional mechanism for disseminating the results of its research and development activities. These results are published by NASA in the NASA STI Report Series, which includes the following report types:

- TECHNICAL PUBLICATION. Reports of completed research or a major significant phase of research that present the results of NASA programs and include extensive data or theoretical analysis. Includes compilations of significant scientific and technical data and information deemed to be of continuing reference value. NASA counterpart of peer-reviewed formal professional papers, but having less stringent limitations on manuscript length and extent of graphic presentations.

- TECHNICAL MEMORANDUM. Scientific and technical findings that are preliminary or of specialized interest, e.g., quick release reports, working papers, and bibliographies that contain minimal annotation. Does not contain extensive analysis.

- CONTRACTOR REPORT. Scientific and technical findings by NASA-sponsored contractors and grantees.

- CONFERENCE PUBLICATION. Collected papers from scientific and technical conferences, symposia, seminars, or other meetings sponsored or co-sponsored by NASA.

- SPECIAL PUBLICATION. Scientific, technical, or historical information from NASA programs, projects, and missions, often concerned with subjects having substantial public interest.

- TECHNICAL TRANSLATION. English-language translations of foreign scientific and technical material pertinent to NASA's mission.

Specialized services that complement the STI Program Office's diverse offerings include creating custom thesauri, building customized databases, organizing and publishing research results ... even providing videos.

For more information about the NASA STI Program Office, see the following:

- Access the NASA STI Program Home Page at ***http://www.sti.nasa.gov***

- E-mail your question via the Internet to help@sti.nasa.gov

- Fax your question to the NASA STI Help Desk at (301) 621-0134

- Phone the NASA STI Help Desk at (301) 621-0390

- Write to:
  NASA STI Help Desk
  NASA Center for AeroSpace Information
  7121 Standard Drive
  Hanover, MD 21076-1320

NASA/CR-2003-212674

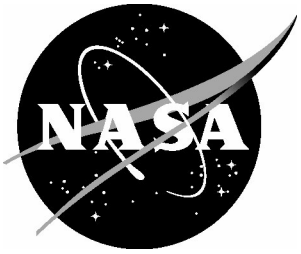

Sound Generation by Aircraft Wake Vortices

Jay C. Hardin
Titan Corporation, Billerica, Massachusetts

Frank Y. Wang
Volpe National Transportation Systems Center, Cambridge, Massachusetts

National Aeronautics and
Space Administration

Langley Research Center
Hampton, Virginia 23681-2199

Prepared for Langley Research Center
under Interagency Agreement IAA-1-600

December 2003

Available from:

NASA Center for AeroSpace Information (CASI)
7121 Standard Drive
Hanover, MD 21076-1320
(301) 621-0390

National Technical Information Service (NTIS)
5285 Port Royal Road
Springfield, VA 22161-2171
(703) 605-6000

SOUND GENERATION BY AIRCRAFT WAKE VORTICES

Jay C. Hardin
Titan Corporation
SRC Division
Billerica, MA 01821

and

Frank Y. Wang
John A. Volpe National Transportation Systems Center
Surveillance and Assessment Division
Cambridge, MA 02142

Abstract

This report provides an extensive analysis of potential wake vortex noise sources that might be utilized to aid in their tracking. Several possible mechanisms of aircraft vortex sound generation are examined on the basis of discrete vortex dynamic models and characteristic acoustic signatures calculated by application of vortex sound theory. It is shown that the most robust mechanisms result in very low frequency infrasound. An instability of the vortex core structure is discussed and shown to be a possible mechanism for generating higher frequency sound bordering the audible frequency range. However, the frequencies produced are still low and cannot explain the reasonably high-pitched sound that has occasionally been observed experimentally. Since the robust mechanisms appear to generate only very low frequency sound, infrasonic tracking of the vortices may be warranted.

TABLE OF CONTENTS

LIST OF FIGURES

Introduction

Wake vortices present a potential hazard to aircraft in the vicinity of airports. For this reason, aircraft operations are scheduled so as to permit the necessary time for the wake vortices of preceding aircraft to either disperse or completely move out of a protective zone based on a worst case scenario. This results in very inefficient use of the existing runway capacities around many airports. If the position of the vortices were known at all times, aircraft operations could then be carried out much more safely and efficiently. One scheme for actively monitoring such vortices is to passively track the acoustic emissions that they produce. This possibility is currently under examination both in terms of the fundamental wake acoustics phenomenology and the operational concept involving such a scheme by the U.S. Government.

In previous acoustic studies within the program, four candidate source mechanisms had been identified to be appropriate for further concentrated examinations:

1. Core vibrations excited by initial conditions or instabilities

2. Unsteady transport of the vortex, including possible interactions with secondary vortices shed from the atmospheric boundary layer

3. Vortex core motion excited by intermittent turbulent structures

4. Unsteady advection of turbulence around the vortex core

It was also stated that the goal of the studies was to determine whether a *unique* signature (one that can be identified in the presence of noise) of a *consistent* dynamic characteristic (one that is present for wake vortices during the time of interest for detecting them) exists. The purpose of this report is to address the aforementioned question. This objective is accomplished by applying classical aeroacoustic theory to engineering vortex dynamic models of these wake phenomena, in order to determine whether a reliable acoustic signal can be identified for tracking purposes.

Vortex Dynamic Models

In order to investigate the sound generation by aircraft wake vortices, engineering models of the phenomena based on the Lagrangian discrete vortex method are developed. Since these phenomena are inherently vortical in nature, vortex method is therefore particularly well suited and very efficient in describing the fundamental fluid mechanics. It is worth noting that engineering models of this type have demonstrated their utility in studies such as NASA's AVOSS program [1]. In addition, these fluid dynamic results can be conveniently integrated with the theory of vortex sound to identify the characteristic acoustic signature associated with the phenomenon.

a. Wake Vortices Interacting with the Ground Plane

The logical first mechanism to explore would be the sound generated by the motion of the vortex pair. After aircraft vortices are fully rolled up, the port and starboard vortices mutually induce each other to move downward until they feel the presence of the ground. As they approach the ground, the increased pressure produced by their interaction with the ground causes the vortices to separate and propagate outward from the aircraft's path. As a model of this phenomenon, consider an initial configuration of two wake vortices of strength Γ and opposite senses of rotation generated by an aircraft of span s at an altitude h as shown in Figure 1:

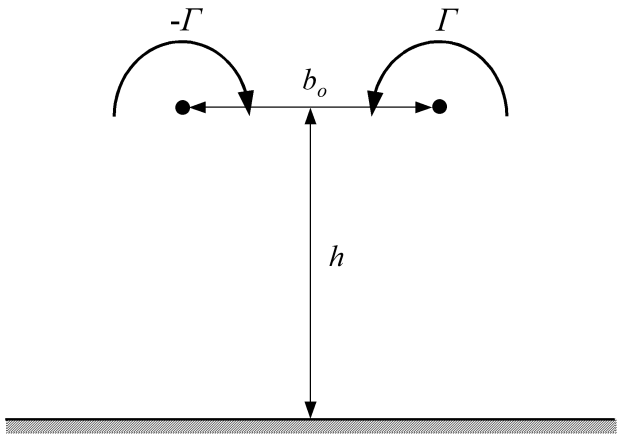

Figure 1: Wake Vortex Model.

It may be of interest to note that experimental evidence has revealed that at a given location along the flight path, the fundamental vortex dynamics can be described as a two-dimensional problem [2], as modeled in Figure 1. The initial separation, b_O, of the vortices has been found to be given by $b_O = (\pi/4)\ s$. The strength of these vortices may also be estimated since the lift per unit span of the aircraft is given by $l = \rho\ U\ \gamma$, where ρ is the density of the air, U is the speed of the aircraft and γ is the circulation per unit length in the wake of the wing. For equilibrium or quasi-equilibrium flights, which are representative of aircraft cruise and landing configurations, the total lift will equal the weight of the aircraft, W. Thus,

$$\Gamma = \frac{4}{\pi}\frac{W}{\rho\ U\ s} \tag{1}$$

where the factor $4/\pi$ stems from the assumed elliptic lift distribution on the wing.

Consider a coordinate system such that one vortex lies at (x, y) and the other at

$(-x, y)$ as shown in Figure 2:

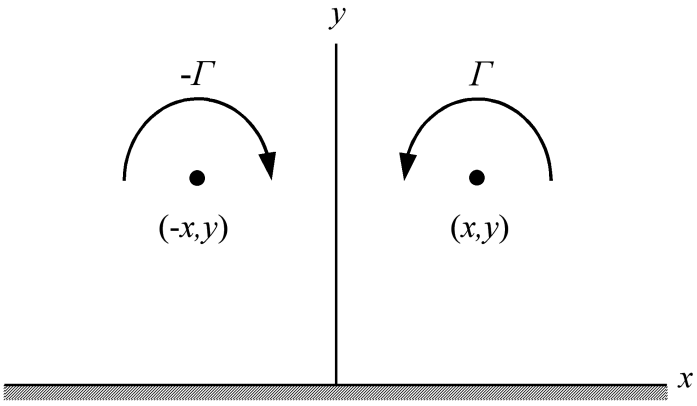

Figure 2: Wake Vortex Coordinate System.

To determine the vortex trajectories, note the initial conditions

$$\begin{aligned} x(0) &= (\pi/8)\ s \\ y(0) &= h \end{aligned} \tag{2}$$

for the vortex in the first quadrant. The presence of the ground plane can be handled by inserting image vortices as shown in Figure 3:

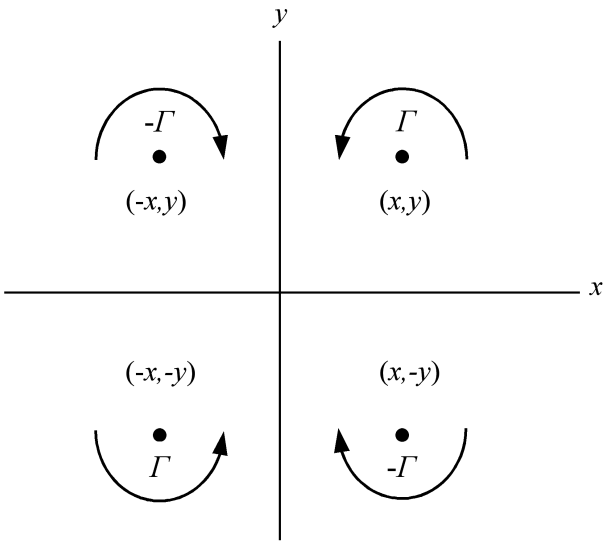

Figure 3: Vortex Image System.

which satisfy the boundary condition that the normal component of the induced velocity field is zero on the ground plane. Then, applying the Biot-Savart Law [3], the velocity components induced on the vortex core in the first quadrant are:

$$\frac{dx}{dt} = \frac{\Gamma}{4\,\pi\,y}\frac{x^2}{(x^2+y^2)}$$
$$\frac{dy}{dt} = \frac{-\Gamma}{4\,\pi\,x}\frac{y^2}{(x^2+y^2)} \qquad (3)$$

This coupled set of nonlinear, first order ordinary differential equations can be simply numerically integrated starting from the initial conditions given by Equation (2) to determine the vortex locations as a function of time. The path of the vortex in the second quadrant is obtained by symmetry. Note that the case of a crosswind can be handled in exactly the same way, by assuming the lateral transport of the vortices advect with the prescribed crosswind profile. The only difference is that the vortices do not remain in mirror image positions and thus a set of four equations must be solved to track both vortices.

As an example under zero crosswind, the case of a B747 with wingspan of 59.7 m, altitude of 150 m, and a constant circulation strength of 595.54 m^2/sec. has been considered. The time step, $\Delta t = 0.5\,\text{sec}$, was employed in conjunction with a second-order numerical integration method. Figure 4 shows the trajectory of the vortex core in the first quadrant in a time frame of 150 seconds.

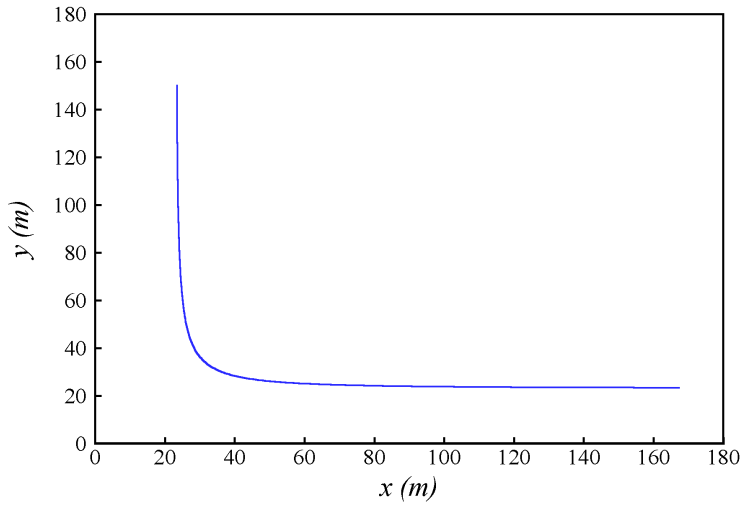

Figure 4: Vortex Path in First Quadrant.

The path of the other vortex is the mirror image about the *y*-axis. The trajectories approach asymptotically to an altitude of 23.4 meters, which represents a height of $b_O / 2$. When the wake is at the aforementioned height, it is considered to be fully in ground effect. Figure 5 displays the vortex positions, *x* and *y*, while Figure 6 displays the vortex velocity components, $u = dx / dt$ and $v = dy / dt$, for the vortex in the first quadrant as a function of time after the vortices are shed from the aircraft. As time goes to infinity,

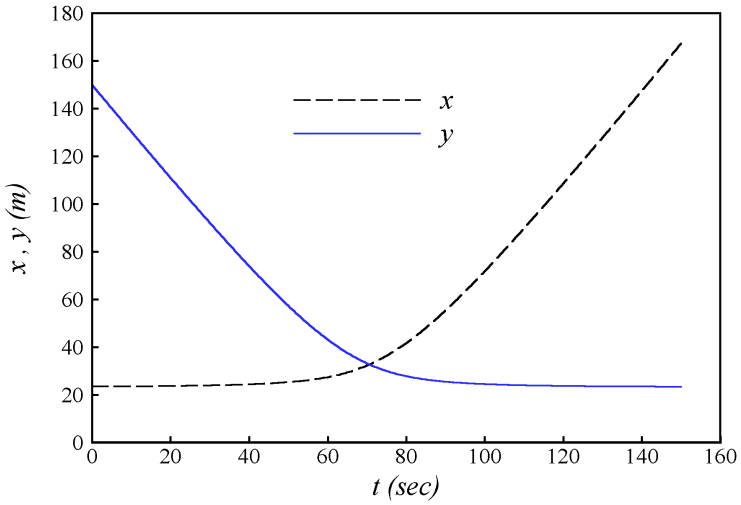

Figure 5: Vortex Position Coordinates.

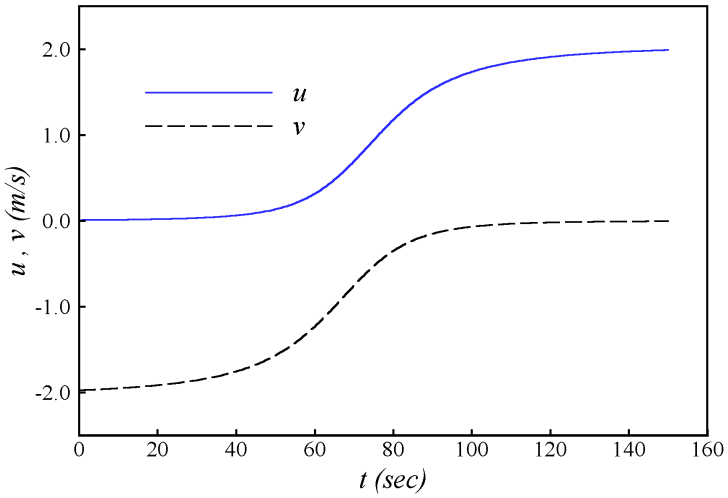

Figure 6: Vortex Core Transport Velocity Components.

the *v* velocity (i.e., vertical component), which initially was -1.97 m/sec goes to zero and the *u* velocity (i.e., horizontal component) asymptotically approaches to a constant value

of 1.99 m/sec., which represents the ground-induced self-propelling vortex velocity. Note that these u and v limiting values take place at the wake altitude of $b_O/2$, and the particular numerical example showed that the process took 70 seconds for the wake to be fully in ground effect. The importance of this time frame will become evident in the subsequent acoustic analysis. Finally, Figure 7 displays the acceleration components du/dt and dv/dt. Both of these acceleration components approach asymptotically to zero as time progresses. These acceleration components are important to the vortex noise generation as will be seen later.

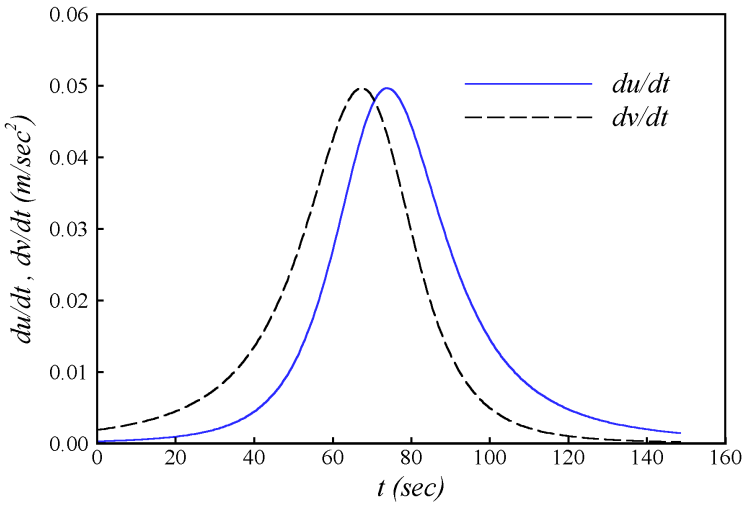

Figure 7: Vortex Core Acceleration Components.

Note that the example has been computed using constant circulation values for both portside and starboard vortices. The process of vortex decay, which would alter the acceleration characteristics, can be prescribed from auxiliary equations. Additional fidelity of the vortex dynamics may include the effects of altitude wind shear, atmospheric boundary layer profile and vortex induced secondary vorticity, whose net effects can all be modeled as discrete vortices. The flow field is then computed using the generalized form of the Biot-Savart Law, by examining the induced velocities from all of physical and the associated image vortices. The associated modeling and numerical issues are beyond the scope of the present study. The aforementioned description is provided for the purpose of emphasizing that higher order wake modeling can be accomplished within the present theoretical framework.

b. Two Unequal Magnitude Vortices in Free Space

The problem of two unequal magnitude vortices of the same sense of rotation in free space was also considered as a model representing one of the wake vortices interacting with an atmospheric eddy, a wind shear, or other airframe vortices such as that of a flap. Consider the coordinate system shown in Figure 8:

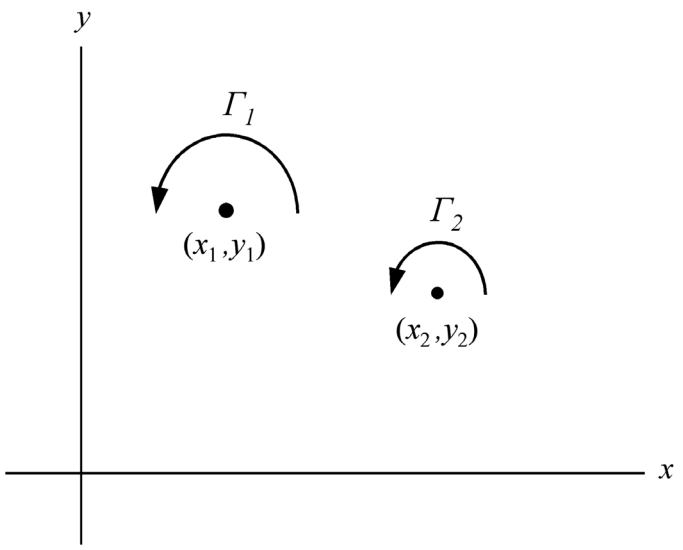

Figure 8: Unequal Vortices Coordinate System.

i.e., a vortex of strength Γ_1 at the position (x_1, y_1) and a vortex of strength Γ_2 at the position (x_2, y_2). Again applying the Biot-Savart Law, the equations governing the system are

$$\begin{aligned}
\frac{dx_1}{dt} &= \frac{\Gamma_2}{2\,\pi\,r^2}(y_2 - y_1) \\
\frac{dy_1}{dt} &= \frac{-\Gamma_2}{2\,\pi\,r^2}(x_2 - x_1) \\
\frac{dx_2}{dt} &= \frac{-\Gamma_1}{2\,\pi\,r^2}(y_2 - y_1) \\
\frac{dy_2}{dt} &= \frac{\Gamma_1}{2\,\pi\,r^2}(x_2 - x_1)
\end{aligned}$$

where $r^2 = (x_2 - x_1)^2 + (y_2 - y_1)^2$ can be shown to be a constant equal to its value at the initial condition. This set of equations may readily be solved by Laplace transformation yielding the solution

$$\begin{aligned}
x_1(t) &= x_1(0) + X_1(t)\cos\theta - Y_1(t)\sin\theta \\
y_1(t) &= y_1(0) + X_1(t)\sin\theta + Y_1(t)\cos\theta \\
x_2(t) &= x_1(0) + X_2(t)\cos\theta - Y_2(t)\sin\theta \\
y_2(t) &= y_1(0) + X_2(t)\sin\theta + Y_2(t)\cos\theta
\end{aligned} \tag{4}$$

where $\cos\theta = \left(x_2(0) - x_1(0)\right)/r$, $\sin\theta = \left(y_2(0) - y_1(0)\right)/r$, and

$$X_1(t) = \frac{B\ r}{A+B} - \frac{B\ r}{A+B}\cos(A+B)\ t$$

$$Y_1(t) = \frac{-B\ r}{A+B}\sin(A+B)\ t$$

$$X_2(t) = \frac{B\ r}{A+B} + \frac{A\ r}{A+B}\cos(A+B)\ t$$

$$Y_2(t) = \frac{A\ r}{A+B}\sin(A+B)\ t$$

where $A = \Gamma_1/(2\ \pi\ r^2)$, $B = \Gamma_2/(2\ \pi\ r^2)$, and the values at time = 0 are the initial conditions. Note that the solution is periodic with frequency $\omega = A + B$ or $f = (A+B)/(2\ \pi)$ as the vortices merely rotate about one another periodically. Since the propagation of acoustic waves is a linear phenomenon, this same frequency will appear in the acoustic field. Some idea of the frequency of this oscillation may be obtained by again considering the case of a B747 where $\Gamma_1 = 595.54$ m^2/sec. Supposing for example that $\Gamma_2 = 0.1 \cdot \Gamma_1$ and $r = 10$ m yields $f =$ 0.16 Hz, a frequency much below human hearing (30 Hz). Even if $r = 1$ m, which would realistically be much too close, the frequency would be only 16 Hz. Thus, this mechanism produces only infrasonic signals and could not be responsible for any periodic signal that might be heard.

As was seen before, the presence of a ground plane can be added into this model quite simply using image vortices. However, then the motion can no longer be solved analytically. The solution is known [4] from previous numerical calculations to exhibit chaotic behavior. Such behavior is not a numerical artifact but is produced by extreme sensitivity to initial conditions. For some sets of initial conditions, the two vortices will continue to oscillate periodically about one another as they are convected by their images in the plane as was seen in the previous analysis of wake vortices in the presence of the ground. For other initial conditions, the two vortices separate as each is convected at different speeds by their image vortices.

Applications of Vortex Sound Theory

The theory of vortex sound generation was first developed by Powell [5] who showed that the primary source of sound generation in low Mach number flows was due to the presence of vorticity, in fact, acceleration of vorticity is the major source. The acoustic pressure, p , was shown to satisfy the wave equation

$$\frac{1}{c^2}\frac{\partial^2 p}{\partial t^2} - \nabla^2 p \cong \rho_o \nabla \cdot (\bar{\omega} \times \bar{v}) \tag{5}$$

Here c and ρ_o are the ambient speed of sound and density respectively and $\bar{\omega}$ and $\bar{v}$ are the vorticity and velocity vectors. Integrating Equation (5) and performing a multipole expansion, which amounts to neglecting retarded time differences across the source distribution, it can be shown [6] that the solution to this equation in free space is given by

$$p(\bar{X},t) \cong \frac{-\rho_o}{4\ \pi\ c^2}\frac{x_i x_j}{\left|\bar{X}\right|^3}\left(\frac{d^2}{dt^2}\int_V y_i\ L_j\ d\bar{y}\right)^* \tag{6}$$

Here $\bar{X} = (x_1, x_2, x_3)$ is the observer position, $\bar{L} = \bar{\omega} \times \bar{v}$ is the Coriolis acceleration vector, V is the volume containing the flow, and the asterisk indicates evaluation at the retarded time $t - \left|\bar{X}\right| / c$.

a. Wake Vortices in Presence of Ground Plane

When the flow takes place in the presence of a surface, one ordinarily expects an additional surface integral [7] to appear in the solution given by Equation (6). However, for the special case of a plane surface, Powell [8] showed that the surface integral is negligible if the image vortices are treated as real and the volume integral taken over both the real and image spaces. Thus, consider the geometry shown in Figure 3 for the case of wake vortices interacting with a ground plane. The vortices have velocities only in the y_1 and y_2 (or x and y) directions, i.e., for the vortex in the first quadrant $\bar{v} = (u, v, 0)$ where u and v are shown on Figure 6. Further, they only have a vorticity component in the y_3 direction, i.e., again for the vortex in the first quadrant $\bar{\omega} = (0, 0, \Gamma\delta(\bar{y} - \bar{y}_v))$ where $\delta(\bullet)$ is the two dimensional Dirac delta function $\delta(x - x_v)\delta(y - y_v)$ and $\bar{y}_v = (x_v, y_v)$ is the vortex position in the $x - y$ plane. Thus, the Coriolis acceleration only has components in the y_1 and y_2 directions, i.e., $\bar{L} = (-\Gamma v\delta(\bar{y} - \bar{y}_v), \Gamma u\delta(\bar{y} - \bar{y}_v), 0)$ for the vortex in the first quadrant. Thus, $\int_V y_i L_3 d\bar{y} = 0$ and, assuming that the coordinate system is placed such that the length l of the vortices extends over $-l/2 \le y_3 \le l/2$, $\int_V y_3 L_i d\bar{y} = 0$. This choice for the origin of the coordinate system not only simplifies the

integrations, but also minimizes the retarded time differences over the length of the source distribution. Carrying out the other 4 integrals over all four (real and image) vortices, paying attention to the positions and signs of both the circulations and velocity components yields

$$\int_V y_1 L_1 dy = -4x\Gamma v l$$
$$\int_V y_1 L_2 dy = \int_V y_2 L_1 dy = 0$$
$$\int_V y_2 L_2 dy = 4y\Gamma u l$$

where x and y are the vortex positions shown in Figure 5. Thus, applying these relations in Equation (6) yields the expression for the acoustic pressure radiated by the vortices

$$p(\overline{X},\, t + |\overline{X}|/c) = \frac{\rho_0\ \Gamma\ l}{\pi\ c^2\ |\overline{X}|^3}\left[x_1^2 \frac{d^2}{dt^2}(xv) - x_2^2 \frac{d^2}{dt^2}(yu)\right] \tag{7}$$

Now, suppose that the observer is on the ground at a distance d from the aircraft flight path and at the center of the vortices' length, i.e., $\overline{X} = (d,0,0)$. Then the expression for the observed acoustic pressure, given by Equation (7), becomes:

$$p(\overline{X},\ \ t + d/c) = \frac{\rho_o\ \ \Gamma\ \ l}{\pi\ \ c^2\ \ d}\frac{d^2}{dt^2}(xv) = \frac{\rho_o \Gamma\ \ l}{\pi\ \ c^2\ \ d}\left[2u\frac{dv}{dt} + x\frac{d^2v}{dt^2} + v\frac{du}{dt}\right]$$

In order for the use of this expression to be precisely valid, the observer should be in the farfield of the source, i.e., the distance d should be large enough that both $d > l$ and $d > \lambda$, where λ is the wavelength of the sound produced. Both of these conditions are often violated in wake vortex noise monitoring. However, all the violation means is that higher order sources may come into play and that the amplitude of the acoustic wave may not fall off like $1/r$. The basic signal characteristics, which are very low in frequency as discussed below, will be preserved.

The normalized acoustic pressure at the observer time $t + d/c$ is given by

$$\frac{\pi\ c^2\ d}{\rho_o\ \Gamma\ l}\, p(\overline{X},\ t + d/c) = \frac{d^2}{dt^2}(xv) = 2u\frac{dv}{dt} + x\frac{d^2v}{dt^2} + v\frac{du}{dt} \tag{8}$$

As an example, the normalized acoustic pressure radiated in the case of a B747, as discussed above, is plotted in Figure 9 as a function of source time t rather than observer time $t + d/c$ for an observer at a distance of $d = 50$ m from the ground track of the aircraft and an initial vortex altitude of $h = 150$ m. The signal has a zero asymptote as time continues and the acceleration of the vortex diminishes. Note that the acoustic signal resembles one cycle of a periodic signal with a period near 45 seconds that would correspond to a frequency near 0.02 Hz, again infrasonic.

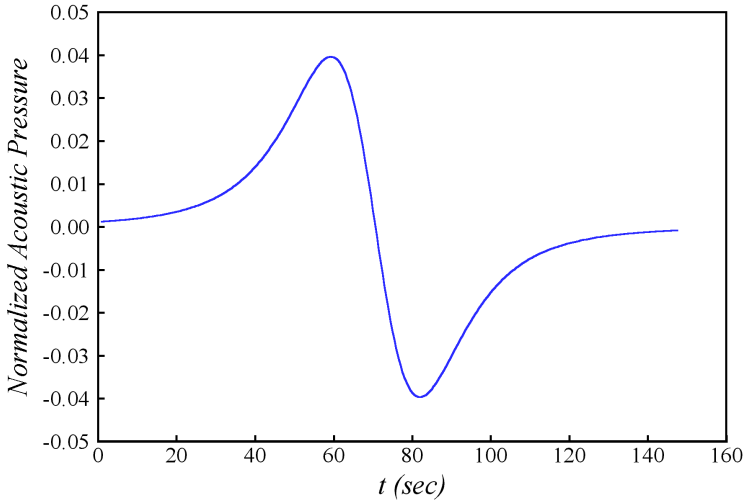

Figure 9: Acoustic Pressure Time History.

b. Elliptic Vorticity Distribution

As an example of a distributed vortex, consider a uniform distribution of vorticity Ω over an elliptical region in free space as shown in Figure 10:

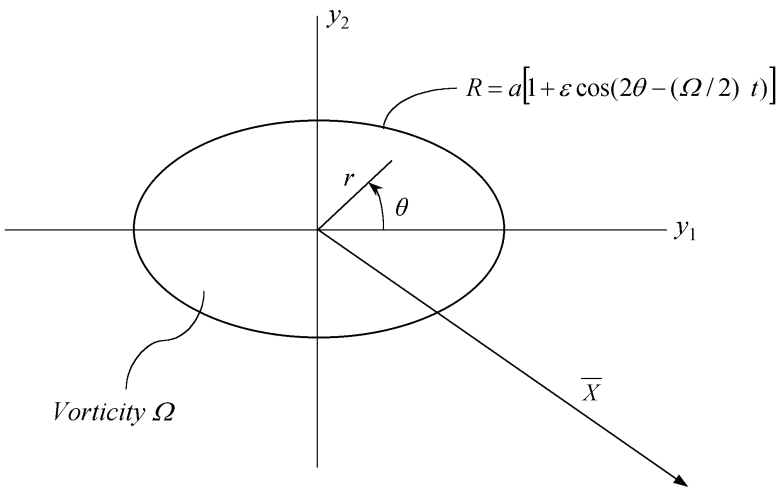

Figure 10: Elliptic Vorticity Distribution.

Wake vortices of this shape have been confirmed via smoke visualization flight tests and this appearance might be due to the influence of the fuselage or wing on the rolling up of wakes. The origin of coordinates is again taken at the center of the vortice's length with the coordinate y_3 in the axial direction. Thus the vorticity vector is given by $\overline{\omega} = \Omega\ \hat{k}$. This vorticity distribution in the infinite length, two dimensional case has been studied by several research workers, including Howe [9], who have shown that the configuration is stable and rotates with angular velocity $d\theta/dt = \Omega/4$ to the order of ε, where ε is the eccentricity of the ellipse. Due to the rotation, the boundary of the vorticity distribution at any time t is given by $r = R = a\left[1 + \varepsilon \cos(2\theta - (\Omega/2)t)\right]$. The velocity vector lies in the plane, i.e., $\overline{v} = u\ \hat{i} + v\ \hat{j}$, where

$$u = \frac{-\Omega\ r}{2}\left[\sin\theta + \varepsilon \sin(\theta - \frac{\Omega}{2}t)\right]$$

$$v = \frac{\Omega\ r}{2}\left[\cos\theta - \varepsilon \cos(\theta - \frac{\Omega}{2}t)\right]$$

Thus, the Coriolis acceleration vector becomes $\overline{L} = -\Omega\ v\ \hat{i} + \Omega\ u\ \hat{j}$, i.e., $\overline{L} = (L_1, L_2, 0)$.

The sound radiated by this vortex motion may be calculated from Equation (6).

Since $L_3 = 0$, $\int_V y_i L_3 d\bar{y} = 0$. Further, due to symmetry, $\int_V y_3 L_j d\bar{y} = 0$. Thus, the necessary integrals, correct to $O(\varepsilon)$, are:

$$\int_V y_1 L_1 dy = -\frac{L\Omega^2 a^4 \pi}{8}(1 + \varepsilon \cos\frac{\Omega}{2}t)$$

$$\int_V y_2 L_2 dy = -\frac{L\Omega^2 a^4 \pi}{8}(1 - \varepsilon \cos\frac{\Omega}{2}t)$$

and

$$\int_V y_1 L_2 dy = \int_V y_2 L_1 dy = -\frac{L\Omega^2 a^4 \pi\ \varepsilon}{8}\sin\frac{\Omega}{2}t$$

where L is the length of the vortex. The observer will again be taken to be in a plane through the origin which lies at the center of the vortex, i.e., $\bar{X} = (x_1, x_2, 0)$, as shown in Figure 10. Utilizing the above integrals in Equation (6) yields an expression for the sound radiated to the observer position

$$p(\bar{X},\ t) = \frac{-\rho_o L\Omega^4 a^4 \varepsilon}{128\ c^2\ \left|\bar{X}\right|^3}\left[(x_1^2 - x_2^2)\cos\frac{\Omega}{2}t + 2x_1 x_2 \sin\frac{\Omega}{2}t\right]^*$$

where, again, the asterisk indicates evaluation at the retarded time $t - \left|\bar{X}\right|/c$. This expression may be simplified somewhat by introducing the polar coordinates $x_1 = \left|\bar{X}\right|\cos\psi$ and $x_2 = \left|\bar{X}\right|\sin\psi$ yielding

$$p(\bar{X},\ t + \left|\bar{X}\right|/c) = \frac{-\rho_o L\Omega^4 a^4 \varepsilon}{128\ c^2\ \left|\bar{X}\right|}\cos\left(2\psi - \frac{\Omega}{2}t\right) \tag{9}$$

Thus, it can be seen that the sound radiated by the rotation of the elliptical

vorticity distribution is periodic with frequency $f = \Omega / 4\pi$. Note that the amplitude of the acoustic pressure is proportional to the ellipse eccentricity ε.

A concept of the importance of this mechanism may be obtained by considering modeling a typical wake vortex by this elliptical vorticity distribution. The area of the ellipse is $A = \pi\ a^2$, again to the order of ε, and the circulation around it is given by $\Gamma = \Omega\ \ A$. Thus, for modeling this situation, it is necessary to take

$$\Omega = \frac{\Gamma}{A} = \frac{\Gamma}{\pi\ a^2}$$

yielding a frequency that is correct to the order ε.

$$f = \frac{\Omega}{4\pi} = \frac{\Gamma}{4\pi^2 a^2}$$

As an example, consider a B747 with $\Gamma = 595.54$ m^2/sec. and $a = 1.19$ m, then $f = 10.76$ Hz. Thus, it can be seen that this elliptical vortex rotation mechanism also produces very low frequencies for typical wake vortices.

Hydrodynamic Pressure Field

Due to the fact that the amplitude and frequency of the sound calculated above were very low, it is of interest to compare this sound field with the hydrodynamic pressure field produced by the vortex. A vortex produces its own pressure field which is carried along with it as it moves. This hydrodynamic pressure field is not acoustic, i.e., it does not propagate as a wave, but will cause a significant pressure fluctuation as it passes over an observer location. For example, it can be shown that the pressure field produced by a line vortex in free space is given by

$$p(r) = p_o - \frac{\rho_o \Gamma^2}{8 \pi^2 r^2}$$

where r is the radial distance from the vortex core center and p_o is the ambient pressure (i.e., stagnation pressure of the atmosphere). Note that the pressure near the vortex is lower than ambient and returns to ambient like $1/r^2$.

For the phenomenon of wake vortices near a surface, for simplicity only one vortex and its image are considered as shown in Figure 11. In addition, zero crosswind is assumed.

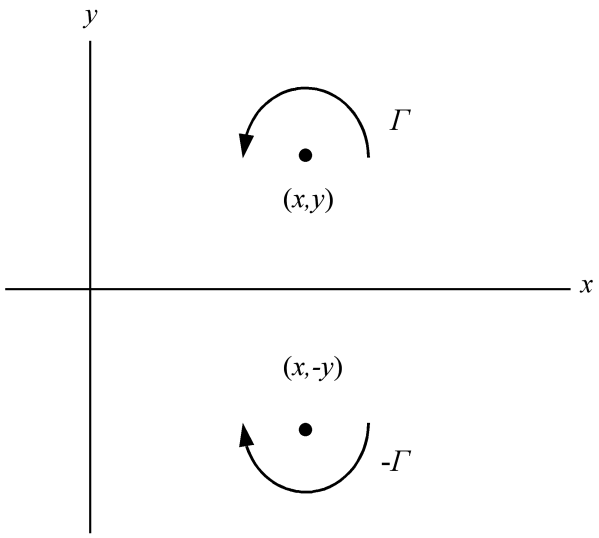

Figure 11: Single Wake Vortex and Its Image.

This model is based on the consideration that over times of interest the vortex will be more influenced by its image than by the wake vortex from the other end of the wing, as its induced velocity becomes negligible. In this case, the vortex is convected by its image at a constant convection velocity, $U_c = \Gamma/(4 \pi y_v)$ where y_v is the constant altitude of the vortex. Recall the example for the B747 shown in Figure 6, where y_v will become $b_o/2$ and U_c approaches to 1.99 m/sec. The observer will be assumed to be on the surface at a distance r from the vortex where the induced velocity components are $u = (\Gamma y_v)/(\pi r^2)$ and $v = 0$ in the x and y directions respectively. The pressure field on the surface may then be shown to satisfy the partial differential equation

$$\frac{\partial}{\partial x}\left[\frac{p}{\rho_o} + \frac{u^2}{2} - uU_c\right] = 0$$

Integrating this equation yields an expression for the deviation of the gauge pressure from ambient on the surface

$$\Delta p(t) = p - p_o = \rho_o u U_c - \frac{\rho_o u^2}{2} \tag{10}$$

Equation (10) has been calculated for the case of a B747, again for an observer at a distance of $d = 50$ m from the ground track of the aircraft, with an initial vortex altitude of $h = 150$ m. and at the center of the vortice's length l, i.e., $\overline{X} = (d,0,0)$. The time history of the hydrodynamic gauge pressure field produced by this calculation is shown in Figure 12, nondimensionalized by the same parameters as were used for the acoustic pressure. The vortex length has been taken as $l = 1000$ m in the nondimensionalization.

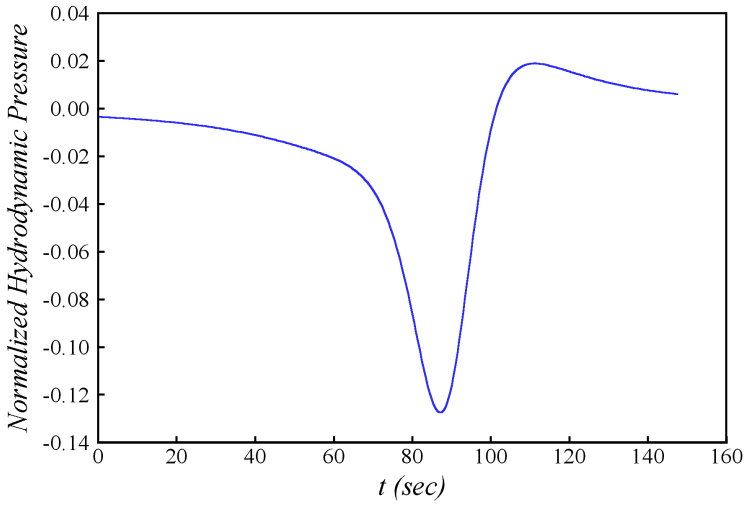

Figure 12: Hydrodynamic Pressure Time History.

Note that the gauge pressure fluctuation is initially negative as the observer feels the low pressure near the core of the vortex. Then, as the vortex passes overhead of the observer position, the pressure fluctuation rises dramatically to an overpressure that then dies off to zero as the vortex is convected away from the observer location. In comparing this hydrodynamic pressure time history with that of the acoustic time history for the same aircraft shown in Figure 9, it can be seen that the hydrodynamic pressure field is several times larger than the acoustic field at this observer location. Further, the hydrodynamic pressure fluctuations occur over nearly the same time interval since the acoustic delay time, d/c, is only 0.15 seconds. Of course, the acoustic field only falls off with distance like $1/r$ while the hydrodynamic field falls off like $1/r^2$. Thus, the acoustic field will eventually become dominant. However, for observer positions such as being used for

monitoring wake vortices near the ground, the hydrodynamic pressure field will dominate.

The dominance of the hydrodynamic pressure field and characteristic signature shown in Figure 12 suggests that measurements of the hydrodynamic pressure field might well be employed to track the vortices. As can be seen, the fundamental frequency of the hydrodynamic pressure field is near 0.01 Hz, similar to that of the acoustic pressure field. Pressure fluctuations with frequencies of this order are readily measured by means of a microbarograph [10] such as are being used to monitor nuclear testing throughout the world. Such pressure transducers are fairly large, on the order of a foot in diameter, and typically have a frequency response that is flat over the interval 0.02-5 Hz. Their response is only 3 dB down at the frequency of interest here, f = 0.01 Hz.

Instabilities

Another mechanism that has been suggested as a possible source of wake vortex noise is the presence of instabilities within the vortex itself. If the vortex were purely two-dimensional, Michalke and Timme [11] have shown that it would be stable by the Rayleigh criterion. However, aircraft wake vortices actually contain a significant axial velocity component, which is explained by first by Batchelor [12] as arising from the competition of circulation-induced pressure gradient and entrained viscous fluid shed by the wing boundary layer into the core. The shear in the axial velocity combined with the vorticity-induced swirl velocity can cause the wake vortex to be unstable to certain types of disturbances as proved by Lessen, Singh and Pallet [13]. They found the vortex to be unstable to non-axisymmetric disturbances with negative azimuthal wavenumbers. The theory of Lessen, Singh and Pallet has been validated by Khorrami and Singer [14] using measurements of the wake vortex produced by a part-span flap. Although they found the instabilities to grow for all negative azimuthal wavenumbers, the data indicated that those with the peak amplification rates, i.e. those in the frequency range

$$2 \le \frac{\omega\ r_o}{U} \le 4 \tag{11}$$

Here U is the mean velocity in the streamwise direction, r_o is the core radius of the vortex and ω is the frequency in radians per second appeared to dominate.

This relation can be applied to the case of aircraft wake vortices in order to estimate the frequencies that might be produced by this instability mechanism. The best data available on wake vortex core radii indicates that the radius may be approximated as $r_o = 0.02\ s$, where s is, again, the span of the aircraft [15]. Taking $U = 66$ m/sec as a typical landing speed, Equation (11) yields the following estimates for aircraft in the commercial fleet:

Table: Predicted Core Radii and Instability Frequencies

Aircraft Type	*Core Radius*	*Frequency Range*
B747	1.19 m	17.6-35.2 Hz
B757	0.76 m	27.6-55.2 Hz
B767	0.95 m	22.1-44.2 Hz
MD80	0.66 m	31.9-63.8 Hz
A320	0.68 m	31.0-62.0 Hz

Since the sound radiation produced by such instabilities satisfies a linear wave equation, the sound radiation will occur at the same frequency as the instability. Note that these predicted frequencies, while mostly audible, are still on the low end of the normal range of human hearing.

The instability mechanism discussed above occurs in incompressible flow. There is also the possibility of a compressible instability since the vortices are formed at altitude where the density is different than that nearer the ground. Since, in the absence of viscous action, vortical fluid tends to remain vortical and vice versa, the vortices would carry the density acquired at altitude with them as they descend allowing buoyancy effects to come into play. Further, it is known that a Kelvin-Helmholtz instability can occur between fluids of differing density and velocity. Such potential instability mechanisms have not been examined as yet.

Conclusion

This report has presented a technical review of the classical theory of vortex noise generation as applied to wake vortex noise generation in support of the wake acoustics research program. Engineering vortex dynamic models were developed for several phenomena that have been considered as possible candidate mechanisms for producing a reliable acoustic signature for tracking purposes. All of the mechanisms considered resulted in low frequency sound generation and suggest that infrasonic tracking of the vortices might be profitably employed. Higher frequency sources would require fluid mechanical mechanisms that oscillate a high frequency, possibly suggesting small scale turbulent phenomena. Such phenomena will be the subject of further research.

Acknowledgement

This work was sponsored by NASA Langley Research Center (NASA LaRC). The authors would like to thank Earl R. Booth and Wayne H. Bryant of NASA LaRC, as well as Robert P. Rudis of the DOT Volpe Center for their support and encouragement.

References

1. Robins, R.E., Delisi, D.P. and Greene, G.C.: Algorithm for Prediction of Trailing Vortex Evolution, *Journal of Aircraft*, Vol.38, No.5, pp. 911-917, 2001.

2. Barker, S.J. and Crow, S.C.: The Motion of Two-Dimensional Vortex Pairs in a Ground Effect, *Journal of Fluid Mechanics*, Vol.82, Pt.4, pp. 659-671, 1977.

3. Batchelor, G.K.: An Introduction to Fluid Dynamics, Cambridge University Press, 1967.

4. Adelman, J.L. and Hardin, J.C.: Vortex Studies Relating to Boundary Layer Turbulence and Noise, *NASA CP 2404*, pp. 25-28, 1985.

5. Powell, A.: Theory of Vortex Sound, *Journal of the Acoustical Society of America*, Vol. 36, No. 1, pp. 177-195, 1964.

6. Hardin, J.C.*:* Analysis of Noise Produced by An Orderly Structure of Turbulent Jets, *NASA TN D-7242*, 1973.

7. Curle, N.: The Influence of Solid Boundaries Upon Aerodynamic Sound, *Proceedings of the Royal Society, Series. A*, Vol. 231, pp.505-514, 1955.

8. Powell, A.: Aerodynamic Sound and the Plane Boundary, *Journal of the Acoustical Society of America*, Vol. 32, pp. 982-990, 1960.

9. Howe, M.S.: Contributions to the Theory of Aerodynamic Sound, with Application to Excess Jet Noise and the Theory of the Flute, *Journal of Fluid Mechanics*, Vol. 71, No.4, pp. 625-673, 1975.

10. Kromer, R.P. and McDonald, T.S.: Report on the Test and Evaluation of the Chaparral Physics Model 4.1.1 Prototype Microbarograph for CTBT Infrasound Array Application, *SAND98-0127*, 1998.

11. Michalke, A. and Timme, A.: On the Inviscid Instability of Certain Two-Dimensional Vortex-Type Flows, *Journal of Fluid Mechanics*, Vol.29, Pt.4, pp. 647-666, 1967.

12. Batchelor, G.K.: Axial Flow in Trailing Line Vortices, *Journal of Fluid Mechanics*, Vol. 20, Pt.4, pp. 645-658, 1964.

13. Lessen, M., Singh, P.J. and Paillet, F.: The Stability of a Trailing Line Vortex, Part 1. Inviscid Theory, *Journal of Fluid Mechanics*, Vol.63, Pt.4, pp. 753-763, 1974.

14. Khorrami, M.R. and Singer, B.A.: Stability Analysis for Noise-Source Modeling of a Part-Span Flap, *AIAA Journal*, Vol.37, No. 10, pp.1206-1212, 1999.

15. Delisi, D.P., Greene, G.C., Robins, R.E. and Wang, F.Y.: Aircraft Wake Vortex Core Size Measurements, *AIAA Paper 2003-3811*, June 2003.

REPORT DOCUMENTATION PAGE

Form Approved
OMB No. 0704-0188

1. REPORT DATE *(DD-MM-YYYY)*	2. REPORT TYPE	3. DATES COVERED *(From - To)*
01- 12 - 2003	Contractor Report	

4. TITLE AND SUBTITLE
Sound Generation by Aircraft Wake Vortices

5a. CONTRACT NUMBER

5b. GRANT NUMBER

5c. PROGRAM ELEMENT NUMBER

6. AUTHOR(S)
Hardin, Jay C.; and Wang, Frank Y.

5d. PROJECT NUMBER
IAA-1-600

5e. TASK NUMBER

5f. WORK UNIT NUMBER
23-137-30-10

7. PERFORMING ORGANIZATION NAME(S) AND ADDRESS(ES)
NASA Langley Research Center
Hampton, VA 23681-2199

Volpe National Transportation Systems Ctr.
Surveillance and Assessment Division
55 Broadway, Kendall Square
Cambridge, MA 02142

8. PERFORMING ORGANIZATION REPORT NUMBER

9. SPONSORING/MONITORING AGENCY NAME(S) AND ADDRESS(ES)
National Aeronautics and Space Administration
Washington, DC 20546-0001

10. SPONSOR/MONITOR'S ACRONYM(S)
NASA

11. SPONSOR/MONITOR'S REPORT NUMBER(S)
NASA/CR-2003-212674

12. DISTRIBUTION/AVAILABILITY STATEMENT
Unclassified - Unlimited
Subject Category 71
Availability: NASA CASI (301) 621-0390 Distribution: Standard

13. SUPPLEMENTARY NOTES
Hardin: Titan Corp.; Wang: Volpe National Trans. Systems Center
An electronic version can be found at http://techreports.larc.nasa.gov/ltrs/ or http://ntrs.nasa.gov
Langley Technical Monitor: Earl R. Booth, Jr.

14. ABSTRACT

This report provides an extensive analysis of potential wake vortex noise sources that might be utilized to aid in their tracking. Several possible mechanisms of aircraft vortex sound generation are examined on the basis of discrete vortex dynamic models and characteristic acoustic signatures calculated by application of vortex sound theory. It is shown that the most robust mechanisms result in very low frequency infrasound. An instability of the vortex core structure is discussed and shown to be a possible mechanism for generating higher frequency sound bordering the audible frequency range. However, the frequencies produced are still low and cannot explain the reasonably high-pitched sound that has occasionally been observed experimentally. Since the robust mechanisms appear to generate only very low frequency sound, infrasonic tracking of the vortices may be warranted.

15. SUBJECT TERMS
Vortex sound; Aircraft wake; Vortex noise

16. SECURITY CLASSIFICATION OF:			17. LIMITATION OF ABSTRACT	18. NUMBER OF PAGES	19a. NAME OF RESPONSIBLE PERSON
a. REPORT	b. ABSTRACT	c. THIS PAGE			STI Help Desk (email: help@sti.nasa.gov)
					19b. TELEPHONE NUMBER *(Include area code)*
U	U	U	UU	28	(301) 621-0390